

Article

Exploring the Land Cover Material Interaction of Urban Open Space on the Thermal Comfort of Crowds in High-Temperature Environments and Retrofit Strategies: Two Case Studies in the Nanjing Xinjiekou District

Ying Tan ^{1,*}, Chen Li ², Haiyi Feng ³ and Junyan Yang ¹¹ School of Architecture, Southeast University, Nanjing 210096, China; yangjunyan@seu.edu.cn² College of Landscape Architecture, Nanjing Forestry University, Nanjing 210037, China; choudoufu@njfu.edu.cn³ Beijing Tsinghua Tongheng Planning Design and Research Institute Co., Ltd., Beijing 100085, China; fenghaiyi@thupdi.com

* Correspondence: 101009917@seu.edu.cn

Abstract: The increased frequency of extreme hot weather events in recent years poses a significant threat to the lives and health of urban residents. Consequently, the thermal comfort of urban open areas has garnered growing attention. The ground material in these urban open areas directly impacts the thermal environment, which significantly influences the comfort of crowds. This study aimed to assess the effect of land cover materials in urban center squares on the thermal comfort of people in high-temperature conditions. Eight types of land cover materials were selected from the two urban squares in the central district of Nanjing Xinjiekou. Physiological equivalent temperature (PET) calculations were performed by measuring the surface temperature, the air temperature, the humidity, and other relevant data to evaluate population thermal comfort. The findings indicated that grass provided the highest thermal comfort, with PET scores ranked as follows, from low to high: grass, permeable bricks, granite, concrete, basalt, bluestone, andesite, and asphalt. Additionally, factors such as color, roughness, and shade within the same material also impacted thermal comfort. Subsequently, using the ENVI-met 5.1 software, surface materials exhibiting superior thermal comfort were simulated for replacement, aiming to confirm the experimental results and propose retrofit strategies for improving urban square thermal comfort by optimizing material selection. The outcomes of this study hold significant implications for urban open space design and the overall well-being of city dwellers. The thermal environment in urban centers during high-temperature conditions can be improved by optimizing the choice of land cover materials in urban open areas, thereby enhancing the comfort of the population.

Keywords: urban open space; land cover materials; thermal comfort; extreme high temperatures; ENVI-met



Citation: Tan, Y.; Li, C.; Feng, H.; Yang, J. Exploring the Land Cover Material Interaction of Urban Open Space on the Thermal Comfort of Crowds in High-Temperature Environments and Retrofit Strategies: Two Case Studies in the Nanjing Xinjiekou District. *Land* **2024**, *13*, 314. <https://doi.org/10.3390/land13030314>

Academic Editor: Rob Roggema

Received: 4 January 2024

Revised: 16 February 2024

Accepted: 26 February 2024

Published: 1 March 2024



Copyright: © 2024 by the authors. Licensee MDPI, Basel, Switzerland. This article is an open access article distributed under the terms and conditions of the Creative Commons Attribution (CC BY) license (<https://creativecommons.org/licenses/by/4.0/>).

1. Introduction

In recent years, the escalation of global climate change has led to frequent and extreme hot weather events, posing substantial threats to the lives and health of urban residents [1]. For example, between 2017 and 2021, the global count of heat-related deaths surged by 68% compared to the preceding five years [2,3]. Within this context, extreme high-temperature weather further worsens the thermal environment in urban open spaces, elevating the thermal risk for those utilizing these areas [4]. Particularly in urban center areas, where a high population density, significant foot traffic, and the widespread use of various artificial surfaces instead of natural ground cover led to increased ground hardening [5,6], combined with the intensification of the urban heat island (UHI) effect, these factors together lead to

the further deterioration of the thermal environment, posing an increasingly severe threat to the thermal comfort of the urban population [7].

Hence, urban center squares, regarded as crucial public open spaces in the city, with a daily foot traffic reaching tens of thousands [8,9], are increasingly receiving attention regarding their thermal comfort. These squares are not only indispensable for residents' outdoor activities but also play a crucial role in promoting physical and mental health [10,11]. Existing studies indicate that the thermal comfort of urban squares is influenced by a variety of factors, including building density and the area and type of vegetation [10,12,13]. Moreover, the surface temperature of the squares is directly affected by the choice of land cover materials and their design [14–16]. Research has demonstrated that selecting appropriate materials or implementing specific technical measures, such as applying surface coatings or enhancing reflectivity, can effectively reduce surface temperatures by approximately 1 °C to 20 °C, thereby significantly improving the local environmental comfort [17,18]. Particularly in conditions of extreme high temperatures, the heat risk for people engaging in outdoor activities significantly increases [1,4], underscoring the pressing need to alleviate the thermal comfort issues in urban squares.

Thermal comfort denotes a state of consciousness reflecting satisfaction with the surrounding thermal environment [19]. Presently, most researchers gauge the impact of thermal environmental parameters—such as temperature, humidity, wind speed, and radiation—on thermal comfort through field measurements conducted in urban squares [20,21]. Subjective evaluations, including questionnaire surveys and other methodologies, have been employed to comprehend human perceptions of diverse thermal environmental conditions and varying levels of acceptance of thermal comfort [22,23]. However, current research primarily concentrates on assessing the effects of green infrastructure and the built environment on the thermal comfort of urban open spaces [22,24–26]. Comparatively, limited attention has been given to studying the influence of land cover materials on thermal comfort within these urban squares, especially in urban center areas significantly affected by high-temperature weather. Previous studies have primarily centered on investigating cool pavements to alleviate the urban heat island effect [27–29]. For instance, some scholars examined reflective pavement, aiming to increase the pavement's albedo, and permeable pavement, targeting increased water retention, thereby altering the pavement's physical and chemical properties to reduce its temperature [30–33].

However, the impact of land cover materials on the thermal comfort of crowds within urban squares remains unclear. Several studies have highlighted the significant role played by ground paving in the overall thermal equilibrium of cities [18,29,34], emphasizing that lowering ground temperatures can substantially enhance the thermal environment of cities during extreme high-temperature conditions. Particularly in cities experiencing continuous high temperatures during the summer, the thermal comfort of the crowd in the city center is under greater threats [35,36].

Therefore, this study aims to explore the impact of land cover materials in urban squares on the thermal comfort of crowds in high-temperature environments. Two representative squares with high urbanization levels, significant foot traffic, and poor thermal comfort in the central area of Nanjing Xinjiekou (Hanzhong Gate Square and Xian Gate Square) were selected as the subjects of this study. Eight common land cover materials were chosen to examine the correlation between different materials and the thermal comfort experienced by the crowds. The experimental results were validated using ENVI-met 5.1, a software commonly used for simulating urban microclimatic environments, and plausible strategies for enhancing thermal comfort were proposed. The objective of this study is to provide a scientific basis for improving thermal comfort in urban squares and to offer sustainable solutions for the planning and design of urban open spaces under summer high-temperature conditions.

The structure of this paper is organized as follows: Section 2 presents the methodology, introducing the study locations and the research period, along with the required measurement data and analysis methods. Section 3 conducts a comparative analysis of the

impact of material type, shadow environment, color, and surface roughness on thermal comfort and validates the results through simulations of the thermal environment of the sites using ENVI-met software. Section 4 delves into the discussion of the research findings, and Section 5 provides a comprehensive conclusion.

2. Materials and Methods

2.1. Study Area

Nanjing is situated between 31°14′–32°36′ N and 118°22′–119°14′ E, serving as one of the central cities in eastern China. Based on the Köppen climate classification system, Nanjing falls under the subtropical humid climate category, characterized by hot summers accompanied by rainfall—a seasonal combination [37,38]. Often referred to as China’s ‘furnace’ city [39], Nanjing experiences summer, as reported by the Nanjing Meteorological Observatory in 2021, lasting from 27 May to 25 September. The hottest months are typically July and August, with an average temperature of 29.74 °C, occasionally reaching maximum temperatures exceeding 40 °C.

As of 1 November 2020, data from the seventh national census of Nanjing shows that the city’s permanent population stands at 9.31 million, with an urban population of 8.08 million. The urbanization rate has reached 86.8%, and the urban population density is 1430 people per square kilometer [40], ranking Nanjing among the top ten Chinese cities in terms of population size and density. This study focuses on two urban open spaces in the Qinhuai District, which covers an area of 49.11 km² and has a population of 740,809, resulting in a density of 15,085 people per square kilometer, the second highest among Nanjing’s eleven districts.

In this study, two city squares in Nanjing, Hanzhong Gate Square and Xian Gate Square, were chosen as experimental sites. The specific location and data pertaining to the parks are detailed in Table 1, while the surrounding land use categories are illustrated in Figure 1 [41]. Both of them fall within the radiation range of the central area of Xinjiekou, Nanjing (as depicted in Figures 2 and 3) [42,43]. Since the beginning of the last century, the Xinjiekou area has functioned as the commercial and comprehensive urban center of Nanjing, characterized by dense population and high commercial activity [44]. It typifies high-density urban center areas, exhibiting characteristics such as a dense population, high urbanization levels, extensive construction, and a significant proportion of paved roads [43,45–47]. Due to the urban heat island effect, temperatures in this area are notably higher than those in the surrounding regions. Consequently, the two city squares within this radiation range serve as ideal research sites.

Table 1. Details of Hanzhong Gate and Xian Gate Squares (Source: authors).

Name	Distance from Xinjiekou Central District	Square Area
Hanzhong Gate Square	1.6 km	29,592 m ²
Xian Gate Square	2.0 km	11,567 m ²

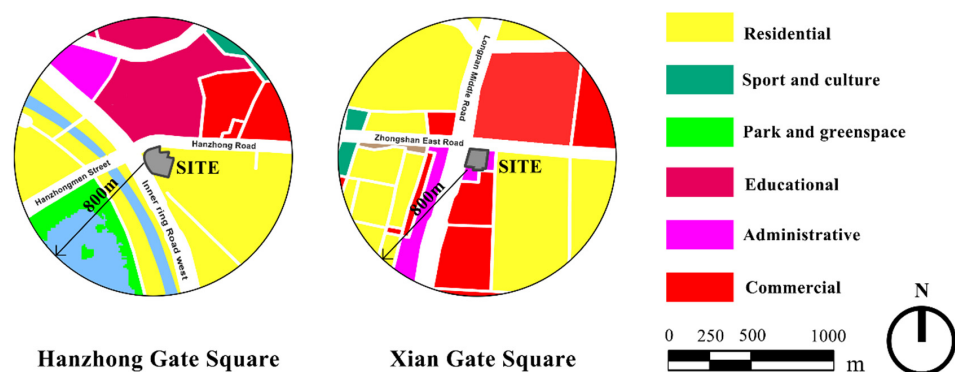


Figure 1. Land use categories surrounding the two squares (Source: authors).



Figure 2. Nanjing City: extent of the Xinjiekou central district and location of the two selected squares (Source: author's archive).



Figure 3. Satellite images of the two selected squares and distance between them (Source: Google maps and author's archive).

2.2. Survey Period

To explore the influence of land cover materials on thermal comfort in high-temperature environments, this study defined high-temperature weather as having a maximum daily temperature exceeding 35 °C [48]. Summer in Nanjing typically spans from June to mid-September [39], with an average temperature of 25.5 °C and a maximum temperature of 39.7 °C recorded in 2021. The outdoor measurement period in this study primarily focused on the high-temperature months during summer, specifically concentrated in mid-to-late June, mid-to-late July, and mid-September. Within these three months—June, July, and September—the author selected four days each month where the daily maximum on-site air

temperature surpassed 35 °C, resulting in a total of 12 days of heat environment data. Each square was surveyed for 2 days per month, summing up to 6 days over the three-month period. Consequently, a total of 12 days of thermal environment data were collected. The specific survey dates are detailed in Table 2. All the thermal environment data in the table were acquired through on-site measurements and represent the average values obtained from all measurement points during the measurement period.

Table 2. Weather conditions (daily averages) during the survey period (Source: authors).

Date	Site	Date Type	Air Temperature (°C)	Relative Humidity (%)	Surface Temperature (°C)	Solar Radiation (w/m ²)	Wind Speed (m/s)
6.20	Hanzhong Gate Square	day off	32.3	46.4	36.4	310.2	1.0
6.23	Hanzhong Gate Square	workday	35.8	32.0	41.4	442.8	1.5
6.27	Xian Gate Square	day off	32.3	62.1	36.4	285.6	1.0
6.29	Xian Gate Square	workday	33.2	58.2	39.6	322.3	0.9
7.11	Hanzhong Gate Square	day off	34.4	57.7	40.6	287.9	1.3
7.18	Xian Gate Square	day off	34.2	59.8	39.7	318.6	1.2
7.19	Hanzhong Gate Square	workday	34.5	58.2	38.8	299.9	1.2
7.20	Xian Gate Square	workday	36.4	56.4	41.7	368.9	1.4
9.17	Xian Gate Square	workday	31.2	54.6	33.5	279.7	0.9
9.19	Hanzhong Gate Square	day off	33.5	59.6	36.4	244.5	1.1
9.22	Han Zhong Gate Square	workday	34.5	46.9	36.7	282.3	1.2
9.25	Xian Gate Square	day off	28.5	70.2	32.6	171.9	1.1

2.3. Data Collection and Analysis

This experiment encompassed various land cover materials commonly utilized in urban squares, such as grass, permeable bricks (travertine), basalt, andesite, concrete, granite, bluestone, and asphalt. Additionally, it involved the classification and analysis of certain hard materials based on their color and surface roughness. During the field investigation conducted at Xian Gate Square and Hanzhong Gate Square, Xian Gate Square was primarily examined to assess different materials, while Hanzhong Gate Square was focused on exploring the impact of varying properties within the same material (i.e., color and surface roughness). Specific measurement points are illustrated in Figure 4.

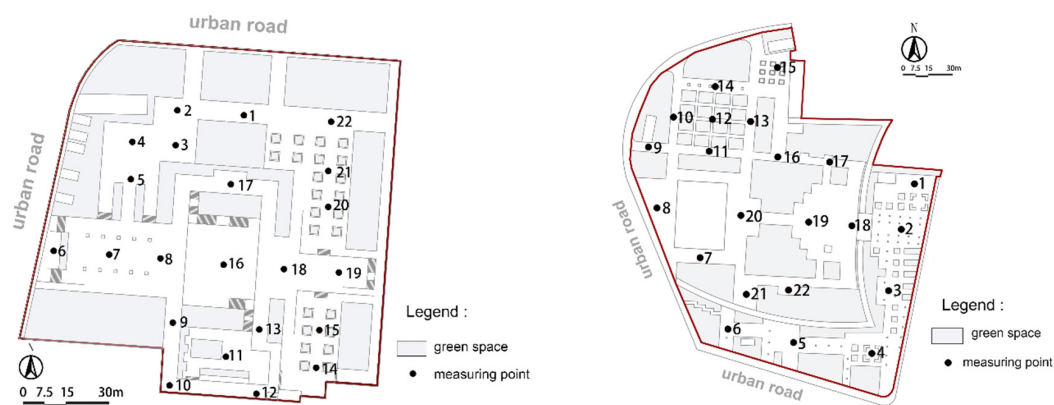


Figure 4. Measurement points (1–22) within each of the two squares (Xian Gate Square and Hanzhong Gate Square) (Source: authors).

Prior to conducting field measurements, an assessment of the site's spatial environment was conducted. Subsequently, 22 measurement points were identified based on factors such as land cover material and shadow conditions (Figure 5). It was ensured that each material type had measurement points directly exposed to sunlight as well as control points to account for other variables. These points were evenly distributed across the site using a grid division method and were conveniently accessible for walkers. All measurement points were located within a circle with a radius of less than 100 m (as illustrated in Figure 6), maintaining consistent microclimate conditions [49].



Figure 5. Measurement points (1–22) on the satellite map (Source: Google maps and author's archive).

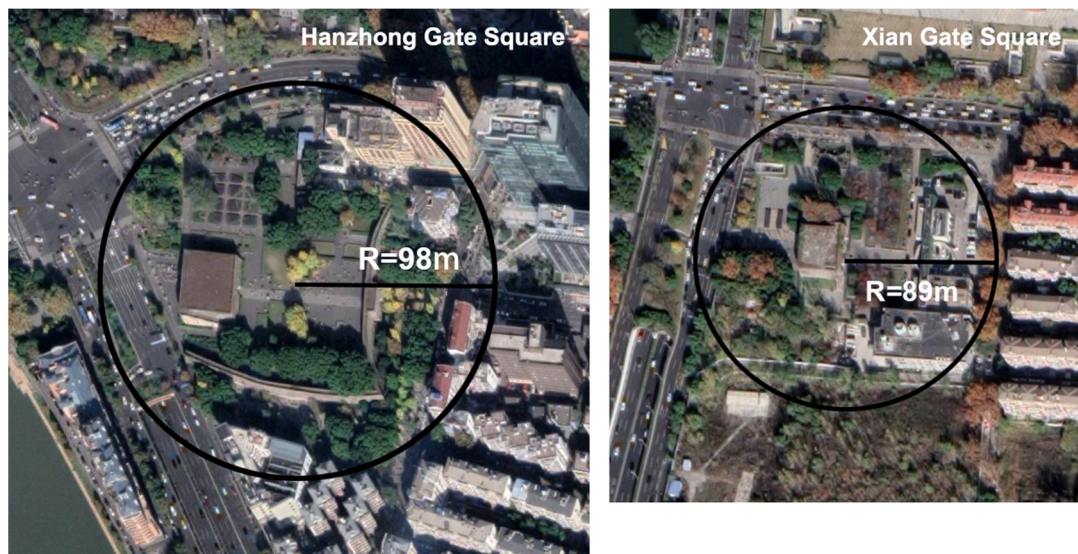






Figure 6. Square measurement points located in a circle with a radius of 100 m (Source: Google maps and author's archive).

The measurements at these points encompassed surface temperature, air temperature, relative humidity, solar radiation, and wind speed. The measurements were taken hourly between 8:00 and 18:00, totaling 11 measurements per day. Points 1 to 22 were divided into four groups, with four surveyors commencing measurements simultaneously. Each

measurement session lasted five minutes to minimize errors due to variations in measurement times. Researchers positioned the measurement instruments at a height of 1.5 m above the ground and spent approximately 10 s at each point. The selection of measurement instruments considered not only their compatibility with the objects being measured but also the measurement method and target, ensuring ease of use in the survey square. Specific parameters of the selected instruments are outlined in Table 3. To synchronize the temperature measuring instrument’s response time and optimize measurement efficiency, measurements were conducted in the sequence of solar irradiance, wind speed, ground temperature, and air temperature.

Table 3. Basic specifications of the instruments used for thermal environment measurements (Source: authors).

Name	Picture	Use	Measuring Range	Unit of Measurement	Precision
Digital hygograph		Measuring air temperature and humidity	−20 °C–60 °C; 0–100% RH	0.1 °C	±0.3 °C
Infrared thermometer		Measuring ground temperature	−50 °C–400 °C	0.1 °C	±1.5 °C
Solar power meter		Measuring solar irradiance	0–2000 W/m ²	0.1 W/m ²	±10 W/m ²
Thermal anemometer		Measuring wind speed	0.1–25.0 m/s	0.01 m/s	±(5% + 1 d)

Additionally, we determined whether the recorded locations were exposed to direct sunlight or situated within shaded areas using Sky View Factor (SVF) calculations. To achieve this, a fisheye lens was attached to the lens of an iPhone 13, capturing images with the lens directed upwards toward the sky from the ground at designated measurement points (refer to Figure 7). These captured images were later analyzed using the RayMan Pro 2 computer model. The analysis provided SVF values spanning from 0 to 1, where a value of 1 indicated complete visibility of the sky.

Based on the field measurement data mentioned above, the physiological equivalent temperature (PET) was employed to assess the thermal comfort experienced of individuals within the city square. PET stands as one of the most extensively used and dependable indices, capable of integrating various elements of the thermal environment to reasonably evaluate human body comfort levels [50]. The RayMan1.2 software was utilized for PET calculation. Survey-acquired data, including temperature, humidity, wind speed, and cloud cover, were batch-imported into the RayMan software for PET value computation. The procedural steps were as follows:

The first step involved importing thermal environment factor data, encompassing air temperature, relative humidity, solar radiation, surface temperature, and wind speed.

The second step entailed inputting spatial and temporal geographic information, specifying the date, time zone, location, latitude, longitude, and altitude.

The third step involved inputting human physiological parameters, such as gender, age, weight, clothing heat resistance, and metabolic rate.



Figure 7. Photographic equipment and captured photographs (Source: authors).

Subsequently, RayMan automatically generated computed results, which were exported for further analysis. The obtained PET values were compared against the PET index comfort ranges (refer to Table 4), revealing the impact of these ranges on thermal comfort. The assessment of human thermal comfort followed the PET interpretation scale proposed by Matzarakis and Mayer [51].

Table 4. PET index ranges and corresponding thermal sensations (Source: authors).

PET (°C)	Thermal Perception	Grade of Physiological Stress
>41	Very hot	Extreme heat stress
35–41	Hot	Strong heat stress
29–35	Warm	Moderate heat stress
23–29	Slightly warm	Slight heat stress
18–23	Comfortable	No thermal stress
13–18	Slightly cool	Slight cold stress
8–13	Cool	Moderate cold stress
4–8	Cold	Strong cold stress
≤4	Very cold	Extreme cold stress

Furthermore, due to the variability of human physiological parameters among individuals, individual counting and calculation can often be challenging. Consequently, standardized data from the China Institute of Standardization were employed for uniform processing. Specifically, the standardized values used for men were 30 years of age, 1.75 m

in height, and 70 kg in weight. Likewise, for women, the standardized values were 30 years of age, 1.70 m in height, and 60 kg in weight.

This study evaluated the impact of different land cover materials on PET values through analysis of variance (ANOVA). Prior to the analysis, a test for homogeneity of variances was conducted to confirm the basic assumptions of ANOVA were met. When ANOVA revealed significant differences ($p < 0.05$) among the materials, we further employed the least significant difference (LSD) test to precisely determine the specific groups among which these differences occur.

2.4. Simulation of the Thermal Comfort in the Squares Using the ENVI-Met Model

ENVI-met stands as a prominent software tool for thermal environment simulation, utilized in more than 50% of thermal environment research studies. This software facilitates efficient three-dimensional simulation of the thermal environment within various spaces. In this study, we aimed to employ ENVI-met to validate whether substituting the current land cover materials in the square with those exhibiting superior thermal comfort, as identified in experiments, will indeed improve the overall environmental thermal comfort. The validation process utilizing the software can be outlined in the following steps:

The initial step involved establishing a three-dimensional simulation model using the latest version of ENVI-met, which is ENVI-met 5.1.1. Model construction commenced by importing satellite images in BMP format at a corresponding scale into the software. Following this, the quantity of model grids was determined in proportion to the actual dimensions, with a grid size set at $50 \times 50 \times 40$, each grid measuring 5 m. The real-world dimensions of the model equated to a length, width, and height of $250 \times 250 \times 200$ m. The simulation location was configured for Nanjing, with the time zone set to UTC + 08:00. Specific foundational modeling parameters are outlined in Table 5 below.

Table 5. Basic modeling parameter settings (Source: authors).

Model Type	Specific Project	Parameters
Basic Model Information	Date	29 June 2021
	Location	Nanjing
	Time zone	UTC+08:00
	Grid Quantity	$50 \times 50 \times 40$
Spatial Element Data	Main Vegetation Index	25 cm tall grass [0100XX]
		High leaf area density trees (15 m) [01OLDM]
	Main Paving Index	High leaf area density trees (5 m) [01OLDS]
		Light-colored granite pavement [0100G2]
Main Structures	Asphalt pavement [0100ST]	
		Han West Gate and Hanzhong Gate Walls [000000]

The first step entailed constructing a three-dimensional model of Hanzhong Gate Square (refer to Figure 8). The second step primarily concentrated on configuring thermal environment parameters. This thermal environment simulation utilized 29 June 2021 as a representative example, chosen due to its exemplification of the poorest thermal comfort experienced during the research period—a typical day characterized by extreme high-temperature conditions in summer. The software simulation necessitated the calculation of average temperature and humidity for each time period based on on-site measurements at all data points. Additional meteorological and environmental parameters are specified in Table 6 below.

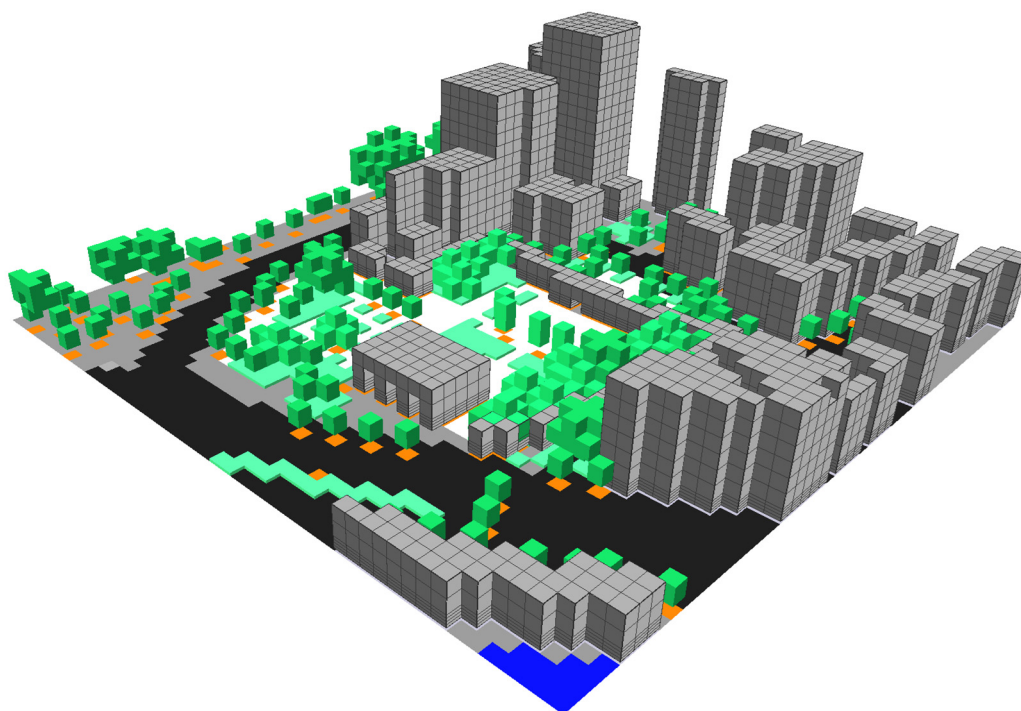


Figure 8. 3D simulation model of Hanzhong Gate Square in ENVI-met (Source: ENVI-met and author’s archive).

Table 6. Meteorological and environmental parameter settings (Source: authors).

Type	Project	Parameters
Meteorological Parameters	Surface Temperature	41.37 °C
	Surface Humidity	32%
	Model Boundary Wind Speed	1.51 m/s
	Wind Direction	Southeast by East (112.5°)
	Minimum Temperature	18.89 °C
	Time of Minimum Temperature	4:00 AM
	Maximum Temperature	39.03 °C
	Time of Maximum Temperature	2:00 PM
	Cloud Cover	High/Medium/Low = 0/0/0
Environmental Parameters	Roughness Length	0.425 m
	Boundary Mode	Force

The assessment of different scenarios utilized the predicted mean vote (PMV) index, an available thermal comfort evaluation metric within ENVI-met. PMV, initially introduced by Fanger in 1972, serves as a classical indicator for evaluating human thermal comfort. It determines the average thermal comfort experienced by individuals within the same environment, estimating it based on four meteorological parameters: air temperature, relative humidity, mean radiant temperature (MRT), and wind speed, alongside considerations of metabolic rate and clothing insulation [52]. PMV is commonly evaluated on a seven-point scale, spanning from −3 (cold) to 3 (hot), with 0 denoting a neutral thermal sensation. Within ENVI-met, PMV can be simulated and analyzed using the BIO-met subprogram.

3. Findings

3.1. Material

Figures 9 and 10 illustrate the measurement outcomes portraying the average surface temperatures of distinct land cover materials and the corresponding air temperature above

the pavement throughout the measurement duration. The surface temperature range observed for the hottest material, asphalt, spans between 34.5 and 60.7 °C, accompanied by an air temperature range between 30 and 39 °C. Conversely, the coolest material, grass, exhibits a maximum surface temperature of 42.2 °C, with an air temperature of 38.3 °C. The difference in surface temperatures among different materials can be as extensive as approximately 20 °C. Notably, the smallest disparities between surface and air temperatures are generally observed early in the morning, while the most significant differences occur during the peak heat of the day.

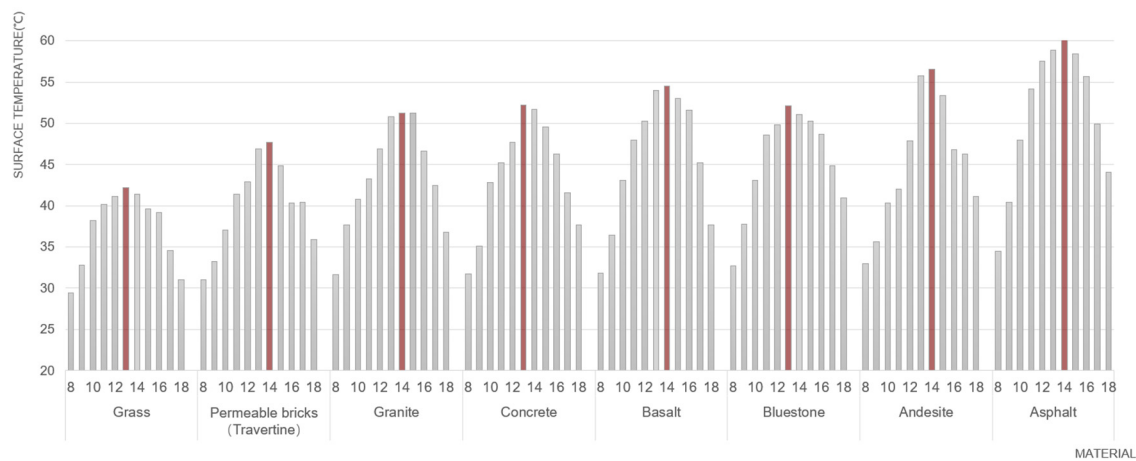


Figure 9. Fluctuations in surface temperature with different land cover materials (Red represents the highest temperature) (Source: authors).

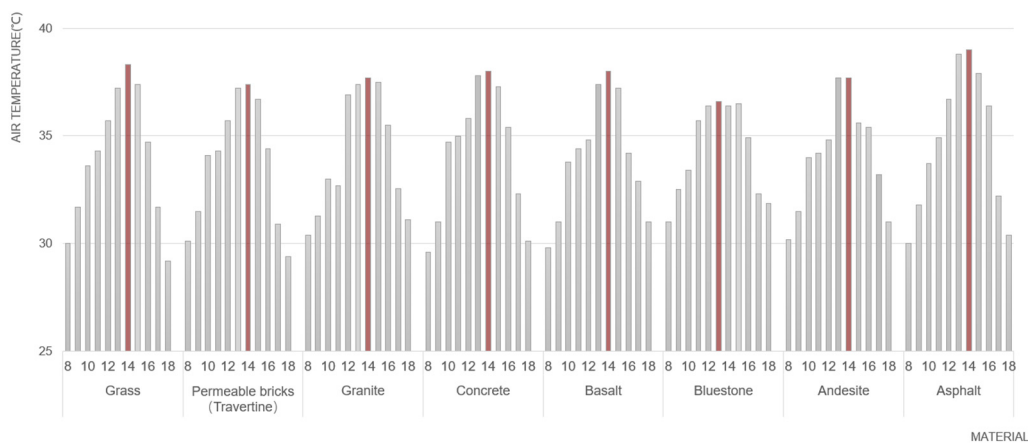


Figure 10. Fluctuations in air temperature with different land cover materials (Red represents the highest temperature) (Source: authors).

Through field measurements, it is evident that both air and surface temperatures generally peak between 12:00 and 15:00 daily. For this study, the author specifically chose to focus on this time frame for more accurately depicting the performance of various land cover materials under extreme high-temperature environmental conditions. During the measurement period from 20 June to 25 September, the average surface temperatures were calculated from 08:00 to 18:00 for the entire duration (total period temperature, TPT) and from 12:00 to 15:00 to capture the hottest part of the day (hottest period temperature, HPT). The data for different materials are specifically presented in Table 7.

Table 7. Surface temperatures of different land cover materials (Source: authors).

Land Cover Materials	Total Period Temperature (°C)	Hottest Period Temperature (°C)
Grass	37.2 °C	41.0 °C
Permeable bricks	40.2 °C	45.6 °C
Granite	43.6 °C	50.0 °C
Concrete	43.8 °C	50.3 °C
Bluestone	45.6 °C	50.8 °C
Basalt	45.9 °C	53.0 °C
Andesite	45.7 °C	53.9 °C
Asphalt	51.1 °C	58.9 °C

The surface temperatures for different materials are ranked based on the hottest calculated values: Asphalt (TPT: 51.1 °C; HPT: 58.9 °C) is the highest, followed by andesite (TPT: 45.7 °C; HPT: 53.9 °C). The temperature ranking descends as follows: basalt (TPT: 45.9 °C; HPT: 53.0 °C), bluestone (TPT: 45.6 °C; HPT: 50.8 °C), and concrete surface (TPT: 43.8 °C; HPT: 50.3 °C). The grass surface (TPT: 37.2 °C; HPT: 41.0 °C) recorded the lowest temperature, significantly lower than the average surface temperature.

Based on the average PET calculated from thermal environmental data for various land cover materials between 08:00 and 18:00 (refer to Figure 11), the grassland (33.91 °C) exhibits a PET score closest to the most comfortable range (18.1–23.0 °C). In contrast, asphalt (45.76 °C), andesite (42.86 °C), basalt (42.17 °C), and bluestone (41.43 °C) fall within the extreme thermal stress zone (>41 °C). A substantial 10 °C disparity in thermal comfort is noticeable between turf and asphalt. Consequently, choosing turf for urban squares instead of materials with poor thermal comfort performance could enhance thermal comfort by up to 10 °C. The ascending order of PET scores, from lowest to highest among the different pavement and surfaces, is as follows: grass (33.91 °C), permeable bricks (36.13 °C), granite (38.12 °C), concrete (38.90 °C), bluestone (41.43 °C), basalt (42.17 °C), andesite (42.86 °C), and asphalt (45.76 °C).

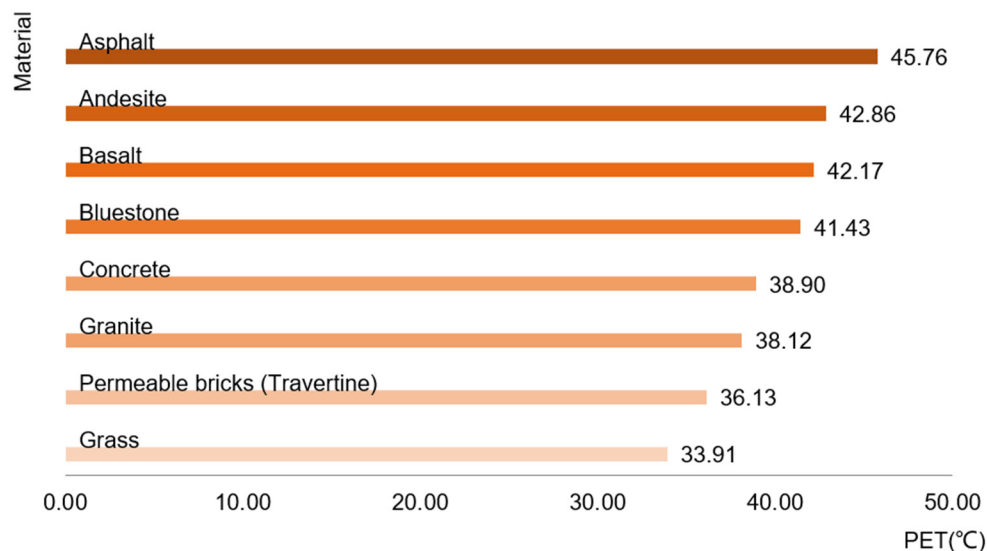


Figure 11. PET values for different land cover materials (Source: authors).

To better illustrate the thermal comfort of various land cover materials under extreme high-temperature conditions, the authors computed PET values for each material between 12:00 and 15:00 (refer to Figure 12), coinciding with the peak temperature. The PET values notably rise across several land cover materials during this hottest time window. Asphalt consistently demonstrates the least favorable thermal comfort performance. Apart from bluestone, which marginally exceeds basalt, the relative ranking of the remaining values remains consistent. The PET values for the total period and the hottest period are shown in Table 8.

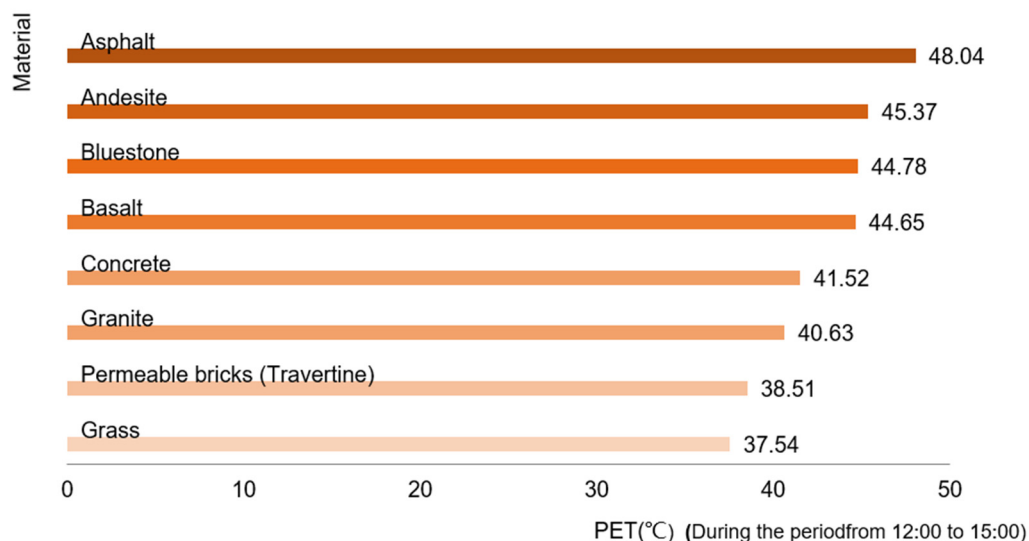


Figure 12. PET values for different land cover materials between 12:00 and 15:00 (Source: authors).

Table 8. Pet values of different materials during the total period and the hottest period (Source: authors).

Land Cover Materials	Total Period PET (°C)	Hottest Period PET (°C)
Grass	33.91 °C	37.54 °C
Permeable bricks	36.13 °C	38.51 °C
Granite	38.12 °C	40.63 °C
Concrete	38.90 °C	41.52 °C
Bluestone	41.43 °C	44.78 °C
Basalt	42.17 °C	44.65 °C
Andesite	42.86 °C	45.37 °C
Asphalt	45.76 °C	48.04 °C

Table 9 presents the results of the statistical analysis. According to the LSD test, the differences in PET scores among various ground cover materials are significant. Asphalt has the highest PET value and is classified into Group A. Following asphalt is andesite, classified into Group AB, then basalt and bluestone, both of which fall into Group ABC. Grass, with the lowest score, is placed in Group E. Slightly higher are permeable bricks and granite, categorized into Groups DE and CDE, respectively. These three, in comparison to asphalt, which has the worst thermal comfort, exhibit significant differences.

Table 9. Least significant difference (LSD) test results of PET scores ($p < 0.05$) (Source: authors).

Land Cover Materials	Least Square Mean					
Asphalt	A					45.7627 °C
Andesite	A	B				42.8613 °C
Basalt	A	B	C			42.1702 °C
Bluestone	A	B	C			41.4337 °C
Concrete		B	C	D		38.8983 °C
Granite			C	D	E	38.1167 °C
Permeable bricks				D	E	36.1267 °C
Grass					E	33.9137 °C

3.2. Shade Condition

To investigate the impact of shadows on land surface temperature, points 4, 5, and 6 in Hanzhong Gate Square and points 6, 7, and 8 in Xian Gate Square were selected for comparison.

Point 4 in Hanzhong Gate Square remains shaded for most of the day, experiencing an average daily sunshine intensity of less than 100 W/m². Point 6 represents a semi-covered

area, receiving sunlight partially throughout the day. Point 5 remains exposed to direct sunlight continuously throughout the day, with all three points featuring light gray, rough granite land cover materials. In Xian Gate Square, Points 6, 7, and 8 depict fully covered, semi-open, and open areas, respectively, with a black, smooth granite land cover material.

Figure 13 displays fisheye photographs taken at each measurement location. The SVF varies across the six measurement locations, ranging from highly shaded—point 4 in Hanzhong Gate Square (SVF = 0.129)—to the unshaded—point 6 in Hanzhong Gate Square (SVF = 0.953).

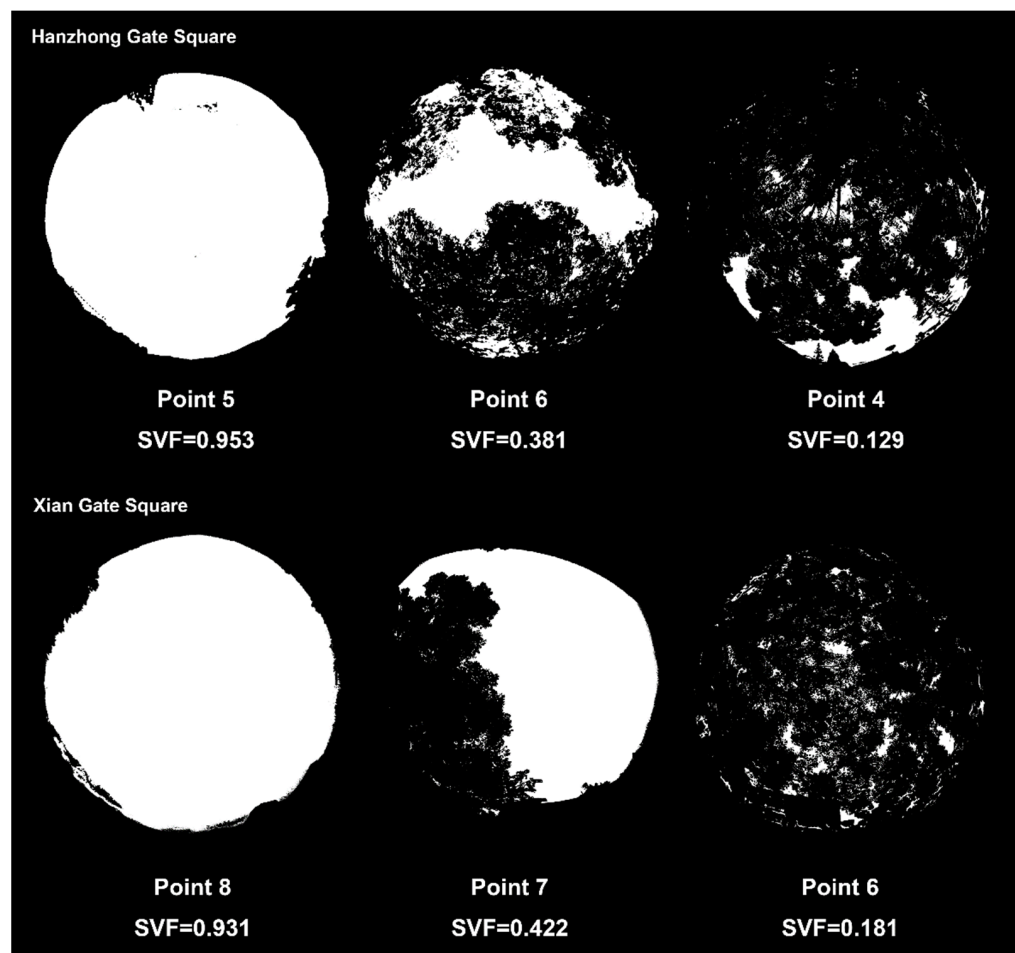


Figure 13. Fisheye photos and SVF analysis results at each location (Source: authors).

Figure 14 displays evident disparities in the surface temperature across corresponding points. The average temperature within the all-day shade or partial shade areas of Hanzhong Gate Square ranges from 36.9–40 °C, markedly lower by 8.9–15.8 °C compared to the point exposed to sunlight throughout the day. The pavement in shaded areas notably exhibits better thermal comfort than those exposed to sunlight, particularly during peak temperatures. The PET difference between the pavements exposed to sunlight and those in shade can reach up to 9.4 °C. This emphasizes not only the significance of land cover materials in optimizing and enhancing the thermal comfort of city squares but also underscores the importance of shade provision from tall trees and structures, along with the appropriate matching of shade conditions with suitable land cover materials, which can significantly alleviate discomfort caused by high temperatures.

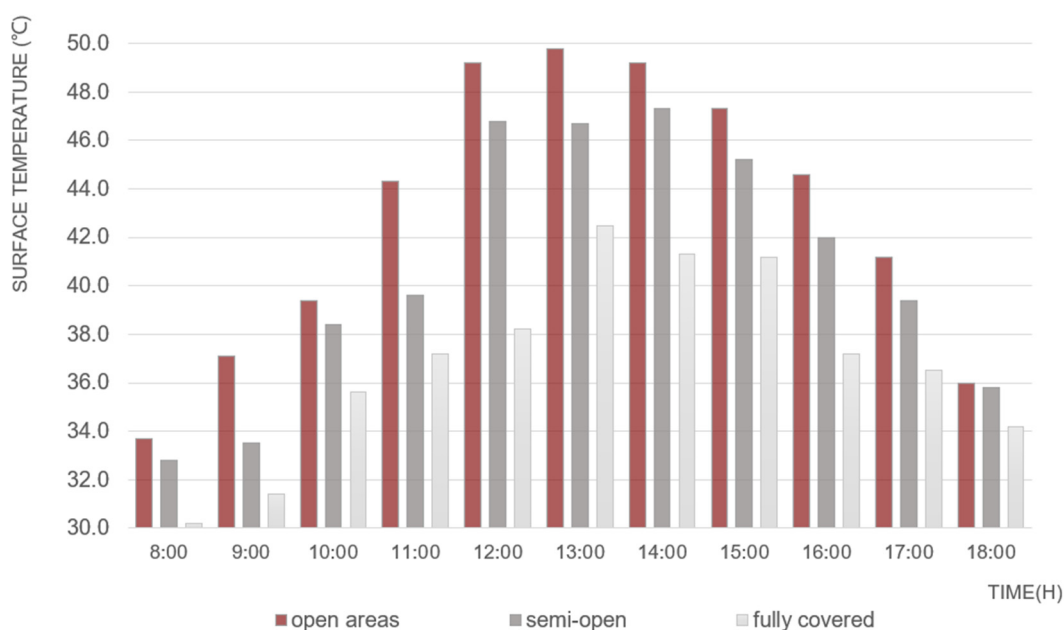


Figure 14. Surface temperature difference between land cover materials under different shade conditions (measurement points 1, 5, and 6 in Hanzhong Gate Square) (Source: authors).

3.3. Color

Comparison of granite pavement of varying colors in Hanzhong Gate Square illustrates the noticeable influence of color on thermal comfort. The granite paving selected for comparison maintained consistent thickness, finish, and lighting conditions, differing solely in color. Figure 15 distinctly illustrates the disparity in surface temperature between point 12 (red smooth granite) and point 11 (black smooth granite) throughout the entire measurement period. On average, black granite records a 3.2 °C higher temperature than red granite; the mean temperature of black smooth granite measures 42.2 °C, while that of red smooth granite records 39.7 °C during the measurement period. During the peak surface temperature period of the day (12:00–15:00), the surface temperature difference can reach up to 4 °C, with a PET difference ranging between 0.9 and 1.8 °C. Similarly, at points 13 and 14 (yellow and red permeable bricks), which share similar lighting conditions, material types, and surface roughness and are in proximity, a discernible effect of color on the surface temperature is evident. The average temperature measured for red permeable bricks is 0.6–1.5 °C higher than that of yellow permeable bricks while maintaining a PET difference within the range of 0.4–1.3 °C between each other.

3.4. Roughness

The measurements indicate that, under identical lighting conditions, pavement samples with matching material types, thicknesses, and colors but varying surface roughness exhibit distinct differences in surface temperatures. For comparison, points 9, 10, and 11 in Hanzhong Gate Square were selected. The temperature of rough granite registers between 0.4 and 2.2 °C higher than that of smooth granite, and the average PET of rough surfaces is approximately 0.57 °C higher compared to smooth surfaces. The rough texture, when contrasted with smooth ground pavement surfaces, diminishes light reflectivity, thereby increasing the probability of light being absorbed upon impact, consequently resulting in higher temperatures on the rough surface in comparison to the smooth surface.

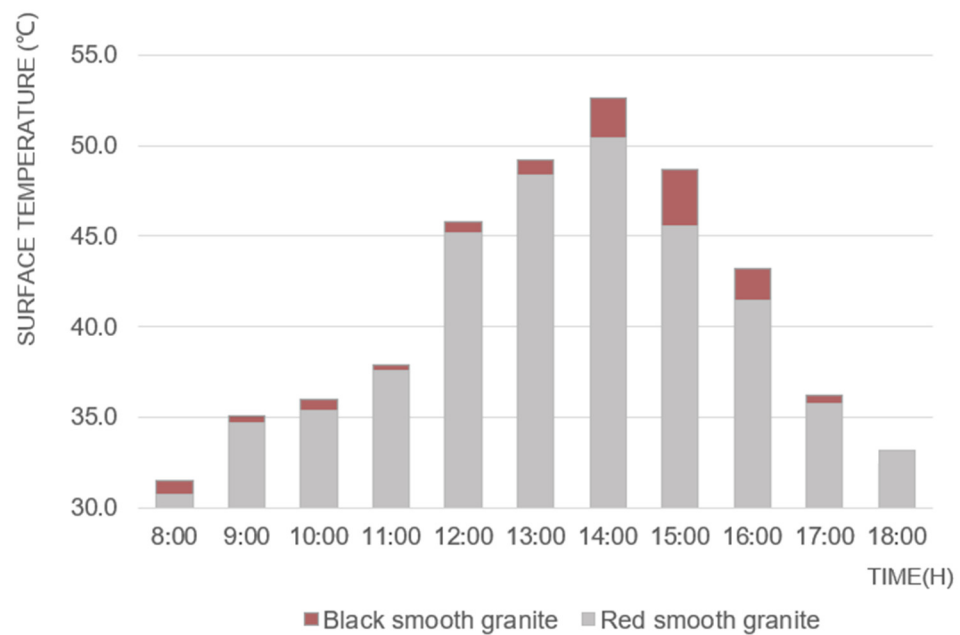


Figure 15. Surface temperature difference between black and red smooth granite (measurement points 9 and 12 in Hanzhong Gate Square) (Source: authors).

3.5. Thermal Comfort Simulation Results from ENVI-Met

In this thermal comfort simulation, seven land cover materials available in the software were primarily selected for further analysis. The types include cement pavement (designated as [0100PG] in ENVI-met), basalt pavement [0100BA], asphalt pavement [0100ST], grass (initially represented by soil [000000] and subsequently overlaid with grass [0100XX]), and three variations of granite pavements distinguished by their color: dark granite pavement [0100GG], gray granite pavement [0100GS], and light-colored granite pavement [0100G2].

Initially, a comparative study was conducted on two models featuring different land cover materials in Hanzhong Gate Square. One model aimed to replicate the original material of the Hanzhong Gate Square, substituting default paving for materials not available in a few software applications. Another model proposed an enhancement strategy based on experimental conclusions to improve the thermal comfort of the square. This involved replacing the original pavement texture with light or gray granite while moderately expanding the lawn area. The specific improvement scheme is illustrated in Figure 16.

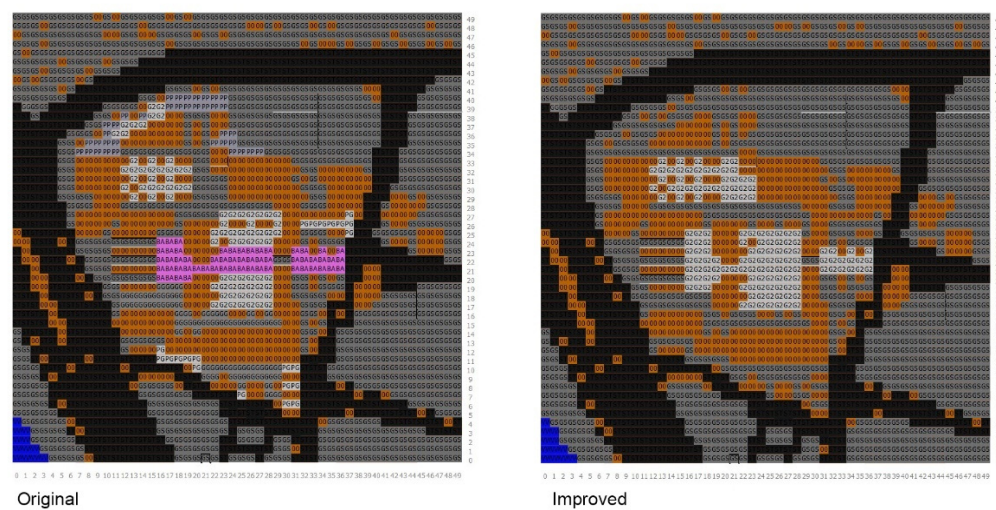


Figure 16. Specific pavement types for both models (Source: ENVI-met and author’s archive).

Compared to the original pavement method, the improvement scheme exhibited an average decrease of 0.012 in PMV during the period from 8:00 to 18:00. Specifically, during the time interval of the poorest thermal comfort, from 12:00 to 16:00, the average PMV decreased by 0.014. The specific PMV values for each time interval are illustrated in Table 10. The thermal comfort situation simulated by the software is shown in Figure 17.

Table 10. PMV values for each time interval in both models. (Source: authors).

Time	Original Pavement (PMV)	Improved Pavement (PMV)
8:00	0.902	0.892
9:00	2.176	2.165
10:00	2.942	2.930
11:00	3.334	3.323
12:00	3.858	3.847
13:00	4.374	4.363
14:00	4.453	4.438
15:00	4.557	4.542
16:00	4.051	4.037
17:00	2.968	2.956
18:00	1.814	1.809

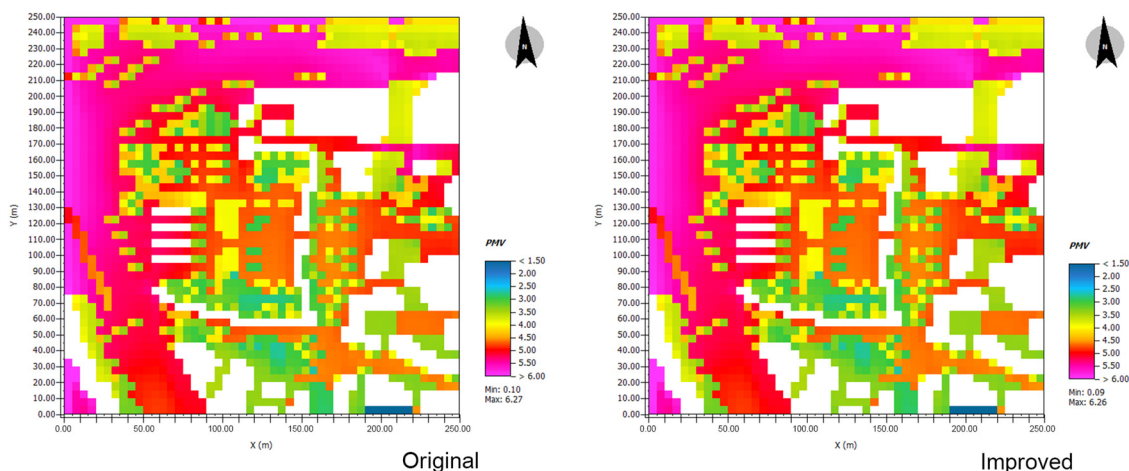


Figure 17. Spatial distribution of PMV in both models at 15:00 (Source: ENVI-met and author’s archive).

Subsequently, simulations were individually conducted for the selected seven-floor land cover materials in the software, resulting in the PMV values for these materials (Figure 18): light-colored granite pavement (PMV = 3.359) > concrete pavement (PMV = 3.297) > asphalt pavement (PMV = 3.294) > basalt pavement (PMV = 3.260) > gray granite pavement (PMV = 3.251) > dark granite pavement (PMV = 3.237) > grass (PMV = 3.030). Smaller PMV values indicate better thermal comfort for individuals. Therefore, grass offers the best thermal comfort, followed by dark granite pavement. To compare the thermal comfort of various land cover materials under extreme high-temperature conditions, PMV values for each material were also evaluated during the hottest period, from 12:00 to 16:00: light-colored granite pavement (PMV = 4.416) > basalt pavement (PMV = 4.350) > concrete pavement (PMV = 4.335) > asphalt pavement (PMV = 4.285) > gray granite (PMV = 4.277) > dark granite pavement (PMV = 4.257) > grass (PMV = 3.993). The specific PMV values for each material are shown in Table 11.

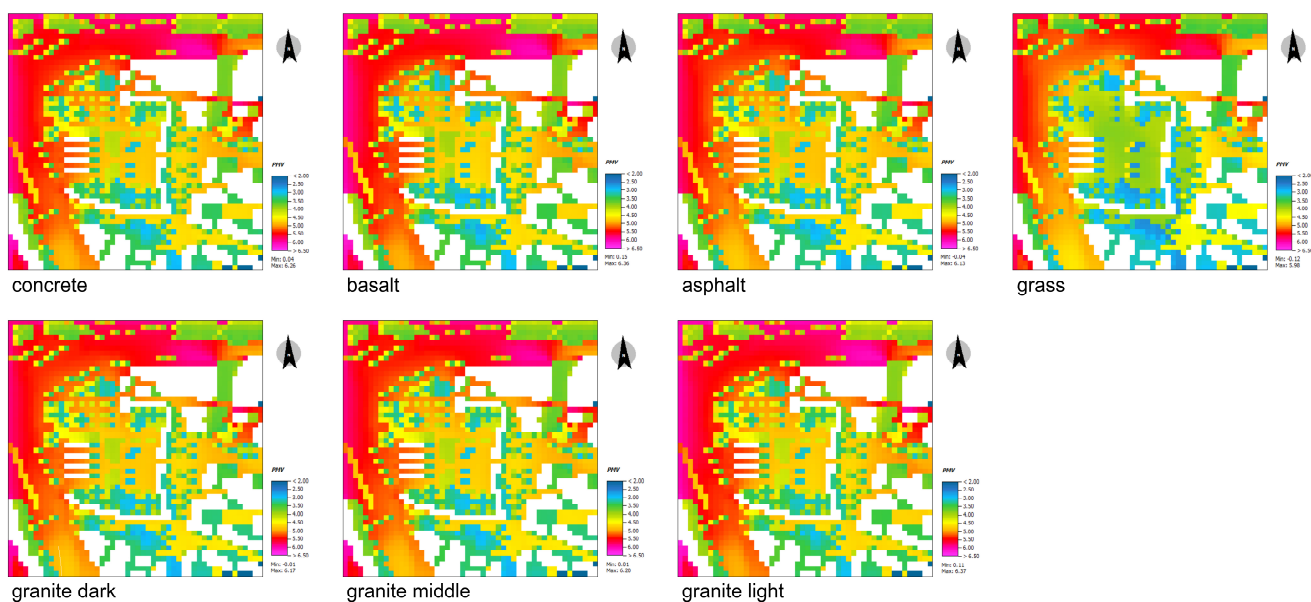


Figure 18. Spatial distribution of PMV for different land cover materials at 15:00 (Source: ENVI-met and author’s archive).

Table 11. PMV values of different land cover materials (Source: authors).

Land Cover Materials	Total Period PMV	Hottest Period PMV
Grass	3.030	3.993
Dark Granite	3.237	4.257
Gray Granite	3.251	4.277
Basalt	3.260	4.350
Asphalt	3.294	4.285
Concrete	3.297	4.335
Light-colored Granite	3.359	4.416

4. Discussion

In extreme high-temperature environments, selecting appropriate land cover materials significantly impacts thermal comfort. This study shows that turf provides superior thermal comfort compared to hard pavements, such as asphalt, andesite, and concrete. Specifically, turf’s PET values were 25.9% lower than those of the material with the poorest thermal comfort, highlighting their potential to enhance urban open spaces’ thermal environment. A further analysis shows that permeable bricks and granite, among hard pavement materials, perform better, with PET value reductions of 21.0% and 16.7%, respectively. Therefore, this study recommends using turf, permeable bricks, or light-colored granite as land cover in urban open spaces to mitigate high temperatures’ adverse effects on thermal comfort.

Our findings indicate that both color and surface roughness contribute to variations in thermal comfort, even with identical materials. The PET value for red granite was 3.5% lower than that for black granite, and the PET value for yellow permeable bricks was 1.7% lower than for red permeable bricks. Additionally, smooth granite surfaces showed a 1.5% decrease in PET values compared to rough surfaces. These results align with previous research, suggesting that the color, texture, and roughness of paving materials affect the levels of heat radiation and conduction [17,53]. However, while considering these factors, it remains crucial to strike a balance with other considerations, such as safety and sustainability. For instance, exploring methods to effectively treat land cover material surfaces to attain optimal thermal comfort without compromising slip resistance and determining suitable colors conducive to psychological and physiological comfort in high-temperature environments merit further investigation in subsequent research.

The impact of direct sunlight on thermal comfort is also evidently significant. Within environments that are fully shaded, the PET values for the same type of paving are 7.1% lower than those in partially shaded environments and 17.4% lower compared to environments fully exposed to direct sunlight. In high-temperature conditions, the shade provided by tall green vegetation can substantially lower surface temperatures, thereby enhancing the thermal comfort of individuals in public spaces [54,55]. Hence, urban planners, when selecting or evaluating land cover materials, it is crucial not only to focus on their thermal characteristics but also to deliberate on integrating shade plants and other structures to create suitable shading and sheltering effects.

In the validation of thermal comfort simulations using ENVI-met software, notable disparities emerged between the simulated results and experimental measurements for specific land cover materials. For instance, concrete and light-colored granite showcased discrepancies: while the software simulations indicated higher thermal comfort for light-colored land cover materials, the actual measurements depicted comparatively lower values. Conversely, asphalt showed lower thermal comfort in simulations but presented relatively higher results in experimental measurements. This inconsistency may stem from the materials chosen for on-site measurements being exposed to direct sunlight, whereas the software simulations encompassed a significant portion of the materials in shaded areas within the square. Light-colored land cover materials, typically possessing lower thermal capacity, tend to heat up more rapidly after absorbing heat. Consequently, they demonstrate relatively poorer thermal comfort in comparison to dark-colored materials.

Some studies suggest that ENVI-met might introduce certain inaccuracies in simulating thermal comfort related to land cover material. Yang et al.'s research also highlights disparities in ENVI-met's simulation of thermal environmental data in urban center spaces compared to actual measurements [56]. Furthermore, various microclimate conditions, surrounding structures, and vegetation in different environments can influence thermal comfort [57,58]. The primary focus of this study is to validate optimization strategies for square pavement using the software. Given the observed deviations between the simulation results and actual measurements, future research requires further exploration. This involves the careful consideration of ENVI-met software model parameters and a more comprehensive examination of the diverse factors influencing thermal comfort in the environment.

We recognize certain limitations in this study, particularly as the research was confined to on-site measurements in two city squares in the center of Nanjing, which may not comprehensively represent all types of urban open spaces. Additionally, given the focus on the high-temperature period during summer, the findings might not be entirely applicable to other seasons or different climatic conditions. Despite these constraints, the challenges posed by extreme high temperatures, especially in regions with cold winters and hot summers, and the thermal comfort issues in high-density urban squares due to high rates of ground hardening and heavy foot traffic underscore the significance of our research. The issues faced by our selected research sites reflect, to a certain extent, a widespread phenomenon. Future research should extend to more cities and various types of urban open spaces, incorporating different climate and seasonal factors to enhance the universality and practicality of the research conclusions.

Furthermore, in the process of calculating the perceived temperature (PET) using Rayman software, we adopted unified human parameters provided by the China Standards Research Institute (a 30-year-old male, 1.75 m tall, weighing 70 kg) to maintain consistency. This approach was aimed at an analysis based on a standardized human thermal comfort response model, facilitating a comparison with research results under other environmental conditions. However, according to our on-site survey, the primary users of Nanjing City Square are middle-aged and elderly women. Relevant studies indicate that middle-aged and elderly individuals are less sensitive to high temperatures, and their tolerance to elevated PET values increases [59,60]. Therefore, in future research, we should consider a more diverse range of population characteristics, such as different ages, genders, and

physiques, to assess thermal comfort and propose more targeted improvement suggestions more accurately.

5. Conclusions

In this study, we selected eight different materials for land covering in urban open spaces to measure relevant thermal environment data and assess thermal comfort during high-temperature weather in summer. The results indicated that the thermal comfort (PET) of turf on pavement was the lowest and closest to the comfortable range, while the PET of asphalt was the highest. The materials, ranked from the lowest PET score to the highest, are as follows: grass (33.9 °C), permeable bricks (36.1 °C), granite (38.1 °C), concrete (38.9 °C), basalt (41.4 °C), bluestone (42.2 °C), andesite (42.9 °C), and asphalt (45.9 °C). Additionally, the study observed that color and roughness had varying effects on thermal comfort, even when the material was consistent.

Furthermore, our study indicates that the same land cover material demonstrates significant variations in its PET values when exposed to direct sunlight. In comparison to pavements situated in shaded areas, those exposed to full sun exhibit an average surface temperature 9–15 °C higher, with temperature differences peaking at 15.8 °C during the hottest period, between 12:00 and 15:00. Additionally, the average PET values in these exposed areas are elevated by 7.8 °C. In the context of urban squares, the strategic planting of green trees or the implementation of shading and relaxation facilities can significantly enhance the thermal comfort of individuals during summer heat, reducing the risk of heat exposure.

In light of these findings, we recommend prioritizing the selection of grass, permeable bricks, or light-colored granite as ground cover materials in the design of modern urban open spaces. Compared to other materials, they can respectively reduce excessively high PET values by up to 25.9%, 21.0%, and 16.7%, significantly improving thermal comfort for people in these spaces. Particularly under frequent extreme high-temperature conditions, the selection of land surface materials for urban open spaces should comprehensively consider safety, aesthetics, thermal comfort, and sustainability.

This study utilized ENVI-met software to assess the potential for enhancing thermal comfort in urban open spaces by selecting improved land cover materials. The feasibility of the retrofit strategies was also verified. In urban center areas characterized by low vegetation coverage and high ground hardness, the influence of ground pavement on the thermal comfort of the public warrants attention. Addressing the urban heat island effect and establishing a favorable thermal comfort environment for urban residents are pressing concerns.

Future research will encompass additional elements within urban open spaces, such as vegetation and relaxation facilities, to explore their combined influence on human thermal comfort in conjunction with different land cover materials. Furthermore, a comprehensive investigation into the thermal comfort of a broader range of land cover materials will be conducted. On-site measurements will be extended to more open spaces in different cities and climate types to broaden the sample size, and data from other seasons will be collected. This effort aims to ensure that research results can be extrapolated to a wider range of conditions, enhancing the overall applicability of the study conclusions. The insights provided by this study aim to offer a scientific basis for urban planning and design to face the challenges of extreme high temperatures, thereby creating a more pleasant and climate-adaptive urban environment.

Author Contributions: Conceptualization, Y.T.; Methodology, Y.T., C.L. and H.F.; Software, C.L. and H.F.; Validation, C.L.; Formal analysis, Y.T. and J.Y.; Investigation, C.L. and H.F.; Resources, Y.T. and H.F.; Data curation, C.L. and H.F.; Writing—original draft, Y.T., C.L. and H.F.; Writing—review & editing, Y.T., C.L. and J.Y.; Visualization, C.L. and H.F.; Supervision, Y.T. and J.Y.; Project administration, Y.T. and J.Y.; Funding acquisition, Y.T. and J.Y. All authors have read and agreed to the published version of the manuscript.

Funding: This research was funded by National Natural Science Foundation of China (grant number: 52378047).

Data Availability Statement: The original contributions presented in the study are included in the article, further inquiries can be directed to the corresponding author.

Conflicts of Interest: Haiyi Feng was employed by the Beijing Tsinghua Tongheng Planning Design and Research Institute Co., Ltd. The remaining authors declare that the research was conducted in the absence of any commercial or financial relationships that could be construed as a potential conflict of interest.

References

1. Ebi, K.L.; Capon, A.; Berry, P.; Broderick, C.; de Dear, R.; Havenith, G.; Honda, Y.; Kovats, R.S.; Ma, W.; Malik, A.; et al. Hot weather and heat extremes: Health risks. *Lancet* **2021**, *398*, 698–708. [[CrossRef](#)] [[PubMed](#)]
2. Papanastasiou, D.; Melas, D.; Kambezidis, H. Air quality and thermal comfort levels under extreme hot weather. *Atmos. Res.* **2015**, *152*, 4–13. [[CrossRef](#)]
3. Jay, O.; Capon, A.; Berry, P.; Broderick, C.; de Dear, R.; Havenith, G.; Honda, Y.; Kovats, R.S.; Ma, W.; Malik, A.; et al. Reducing the health effects of hot weather and heat extremes: From personal cooling strategies to green cities. *Lancet* **2021**, *398*, 709–724. [[CrossRef](#)] [[PubMed](#)]
4. Huang, X.; Yao, R.; Xu, T.; Zhang, S. The impact of heatwaves on human perceived thermal comfort and thermal resilience potential in urban public open spaces. *Build. Environ.* **2023**, *242*, 110586. [[CrossRef](#)]
5. Yang, J.; Wang, Z.-H.; Kaloush, K.E.; Dylla, H. Effect of pavement thermal properties on mitigating urban heat islands: A multi-scale modeling case study in Phoenix. *Build. Environ.* **2016**, *108*, 110–121. [[CrossRef](#)]
6. Yin, Q.; Cao, Y.; Sun, C. Research on outdoor thermal comfort of high-density urban center in severe cold area. *Build. Environ.* **2021**, *200*, 107938. [[CrossRef](#)]
7. Lai, D.; Lian, Z.; Liu, W.; Guo, C.; Liu, W.; Liu, K.; Chen, Q. A comprehensive review of thermal comfort studies in urban open spaces. *Sci. Total. Environ.* **2020**, *742*, 140092. [[CrossRef](#)]
8. Chen, Y.; Liu, T.; Liu, W. Increasing the use of large-scale public open spaces: A case study of the North Central Axis Square in Shenzhen, China. *Habitat Int.* **2016**, *53*, 66–77. [[CrossRef](#)]
9. Lee, J.M. Exploring Walking Behavior in the Streets of New York City Using Hourly Pedestrian Count Data. *Sustainability* **2020**, *12*, 7863. [[CrossRef](#)]
10. Chen, L.; Wen, Y.; Zhang, L.; Xiang, W.-N. Studies of thermal comfort and space use in an urban park square in cool and cold seasons in Shanghai. *Build. Environ.* **2015**, *94*, 644–653. [[CrossRef](#)]
11. Wang, H.; Dai, X.; Wu, J.; Wu, X.; Nie, X. Influence of urban green open space on residents' physical activity in China. *BMC Public Health* **2019**, *19*, 1093. [[CrossRef](#)]
12. Stocco, S.; Cantón, M.A.; Correa, E.N. Design of urban green square in dry areas: Thermal performance and comfort. *Urban For. Urban Green.* **2015**, *14*, 323–335. [[CrossRef](#)]
13. Da Silva, S.; Weruska, P.; Duarte, D.; Pauleit, S. The Role of the Design of Public Squares and Vegetation Composition on Human Thermal Comfort in Different Seasons a Quantitative Assessment. *Land* **2023**, *12*, 427. [[CrossRef](#)]
14. Li, H.; Harvey, J.; Kendall, A. Field measurement of albedo for different land cover materials and effects on thermal performance. *Build. Environ.* **2013**, *59*, 536–546. [[CrossRef](#)]
15. Xiao, H.; Kopecká, M.; Guo, S.; Guan, Y.; Cai, D.; Zhang, C.; Zhang, X.; Yao, W. Responses of Urban Land Surface Temperature on Land Cover: A Comparative Study of Vienna and Madrid. *Sustainability* **2018**, *10*, 260. [[CrossRef](#)]
16. Liu, F.; Zhang, X.; Murayama, Y.; Morimoto, T. Impacts of Land Cover/Use on the Urban Thermal Environment: A Comparative Study of 10 Megacities in China. *Remote Sens.* **2020**, *12*, 307. [[CrossRef](#)]
17. Benrazavi, R.S.; Dola, K.B.; Ujang, N.; Benrazavi, N.S. Effect of pavement materials on surface temperatures in tropical environment. *Sustain. Cities Soc.* **2016**, *22*, 94–103. [[CrossRef](#)]
18. Wu, H.; Sun, B.; Li, Z.; Yu, J. Characterizing thermal behaviors of various pavement materials and their thermal impacts on ambient environment. *J. Clean. Prod.* **2018**, *172*, 1358–1367. [[CrossRef](#)]
19. Mishra, A.K.; Ramgopal, M. Field Studies on Human Thermal Comfort—An Overview. *Build. Environ.* **2013**, *64*, 94–106. [[CrossRef](#)]
20. Lenzholzer, S. Research and design for thermal comfort in Dutch urban squares. *Resour. Conserv. Recycl.* **2012**, *64*, 39–48. [[CrossRef](#)]
21. Xi, T.; Li, Q.; Mochida, A.; Meng, Q. Study on the outdoor thermal environment and thermal comfort around campus clusters in subtropical urban areas. *Build. Environ.* **2012**, *52*, 162–170. [[CrossRef](#)]
22. Zölch, T.; Rahman, M.A.; Pfeleiderer, E.; Wagner, G.; Pauleit, S. Designing public squares with green infrastructure to optimize human thermal comfort. *Build. Environ.* **2019**, *149*, 640–654. [[CrossRef](#)]
23. Jin, Y.; Jin, H.; Kang, J. Combined effects of the thermal-acoustic environment on subjective evaluations in urban squares. *Build. Environ.* **2020**, *168*, 106517. [[CrossRef](#)]

24. De Quadros, B.M.; Mizgier, M.G.O. Urban Green Infrastructures to Improve Pedestrian Thermal Comfort: A Systematic Review. *Urban For. Urban Green*. **2023**, *88*, 128091. [[CrossRef](#)]
25. Ali, S.B.; Patnaik, S. Thermal comfort in urban open spaces: Objective assessment and subjective perception study in tropical city of Bhopal, India. *Urban Clim*. **2018**, *24*, 954–967. [[CrossRef](#)]
26. Deng, X.; Nie, W.; Li, X.; Wu, J.; Yin, Z.; Han, J.; Pan, H.; Lam, C.K.C. Influence of built environment on outdoor thermal comfort: A comparative study of new and old urban blocks in Guangzhou. *Build. Environ*. **2023**, *234*, 110133. [[CrossRef](#)]
27. Qin, Y. A review on the development of cool pavements to mitigate urban heat island effect. *Renew. Sustain. Energy Rev*. **2015**, *52*, 445–459. [[CrossRef](#)]
28. Wang, C.; Wang, Z.-H.; Kaloush, K.E.; Shacat, J. Cool pavements for urban heat island mitigation: A synthetic review. *Renew. Sustain. Energy Rev*. **2021**, *146*, 111171. [[CrossRef](#)]
29. Faragallah, R.N.; Ragheb, R.A. Evaluation of thermal comfort and urban heat island through cool paving materials using ENVI-Met. *Ain Shams Eng. J*. **2022**, *13*, 101609. [[CrossRef](#)]
30. Mohajerani, A.; Bakaric, J.; Jeffrey-Bailey, T. The urban heat island effect, its causes, and mitigation, with reference to the thermal properties of asphalt concrete. *J. Environ. Manag*. **2017**, *197*, 522–538. [[CrossRef](#)] [[PubMed](#)]
31. Kyriakodis, G.-E.; Santamouris, M. Using reflective pavements to mitigate urban heat island in warm climates—Results from a large scale urban mitigation project. *Urban Clim*. **2018**, *24*, 326–339. [[CrossRef](#)]
32. Xie, N.; Li, H.; Abdelhady, A.; Harvey, J. Laboratorial investigation on optical and thermal properties of cool pavement nano-coatings for urban heat island mitigation. *Build. Environ*. **2019**, *147*, 231–240. [[CrossRef](#)]
33. Wang, J.; Meng, Q.; Tan, K.; Zhang, L.; Zhang, Y. Experimental investigation on the influence of evaporative cooling of permeable pavements on outdoor thermal environment. *Build. Environ*. **2018**, *140*, 184–193. [[CrossRef](#)]
34. Taleghani, M.; Berardi, U. The effect of pavement characteristics on pedestrians’ thermal comfort in Toronto. *Urban Clim*. **2018**, *24*, 449–459. [[CrossRef](#)]
35. Pantavou, K.; Theoharatos, G.; Mavrikakis, A.; Santamouris, M. Evaluating thermal comfort conditions and health responses during an extremely hot summer in Athens. *Build. Environ*. **2011**, *46*, 339–344. [[CrossRef](#)]
36. Su, Y.; Wang, C.; Li, Z.; Meng, Q.; Gong, A.; Wu, Z.; Zhao, Q. Summer Outdoor Thermal Comfort Assessment in City Squares—A Case Study of Cold Dry Winter, Hot Summer Climate Zone. *Sustain. Cities Soc*. **2024**, *101*, 105062. [[CrossRef](#)]
37. Yang, X.; Yao, L.; Jin, T.; Peng, L.L.; Jiang, Z.; Hu, Z.; Ye, Y. Assessing the thermal behavior of different local climate zones in the Nanjing metropolis, China. *Build. Environ*. **2018**, *137*, 171–184. [[CrossRef](#)]
38. Du, P.; Chen, J.; Bai, X.; Han, W. Understanding the seasonal variations of land surface temperature in Nanjing urban area based on local climate zone. *Urban Clim*. **2020**, *33*, 100657. [[CrossRef](#)]
39. Tang, C.-S.; Shi, B.; Gao, L.; Daniels, J.L.; Jiang, H.-T.; Liu, C. Urbanization effect on soil temperature in Nanjing, China. *Energy Build*. **2011**, *43*, 3090–3098. [[CrossRef](#)]
40. Fan, Z.; Yanjie, J.; Huitao, L.; Yuqian, Z.; Blythe, P.; Jialiang, F. Travel satisfaction of delivery electric two-wheeler riders: Evidence from Nanjing, China. *Transp. Res. Part A Policy Pract*. **2022**, *162*, 253–266. [[CrossRef](#)]
41. Gong, P.; Chen, B.; Li, X.; Liu, H.; Wang, J.; Bai, Y.; Chen, J.; Chen, X.; Fang, L.; Feng, S.; et al. Mapping essential urban land use categories in China (EULUC-China): Preliminary results for 2018. *Sci. Bull*. **2020**, *65*, 182–187. [[CrossRef](#)]
42. Yang, J.; Shi, X. Coupling Analysis of the Thermal Environment and Spatial Form Unit in Xinjiekou Central Area. In *The Centre of City: Thermal Environment and Spatial Morphology*; Springer: Singapore, 2020; pp. 97–126.
43. Shi, B.; Yang, J. Scale, distribution, and pattern of mixed land use in central districts: A case study of Nanjing, China. *Habitat Int*. **2015**, *46*, 166–177. [[CrossRef](#)]
44. Hu, X.; Zhang, G.; Shi, Y.; Yu, P. How Information and Communications Technology Affects the Micro-Location Choices of Stores on On-Demand Food Delivery Platforms: Evidence from Xinjiekou’s Central Business District in Nanjing. *ISPRS Int. J. Geo-Inf*. **2024**, *13*, 44. [[CrossRef](#)]
45. Yang, J.; Zhu, J.; Sun, Y.; Zhao, J. Delimitating Urban Commercial Central Districts by Combining Kernel Density Estimation and Road Intersections: A Case Study in Nanjing City, China. *ISPRS Int. J. Geo-Inf*. **2019**, *8*, 93. [[CrossRef](#)]
46. Yang, J.; Shi, X. On-Site Measurement and Simulation of the Thermal Environment in Xinjiekou Central Area of Nanking. In *The Centre of City: Thermal Environment and Spatial Morphology*; Springer: Singapore, 2020; pp. 67–95.
47. Hu, X.; Shen, X.; Shi, Y.; Li, C.; Zhu, W. Multidimensional Spatial Vitality Automated Monitoring Method for Public Open Spaces Based on Computer Vision Technology: Case Study of Nanjing’s Daxing Palace Square. *ISPRS Int. J. Geo-Inf*. **2024**, *13*, 48. [[CrossRef](#)]
48. Mearns, L.O.; Katz, R.W.; Schneider, S.H. Extreme High-Temperature Events: Changes in their probabilities with Changes in Mean Temperature. *J. Clim. Appl. Meteorol*. **1984**, *23*, 1601–1613. [[CrossRef](#)]
49. Evyatar, E.; Pearlmutter, D.; Williamson, T. *Urban Microclimate: Designing the Spaces between Buildings*; Routledge: Abingdon-on-Thames, UK, 2012.
50. Höpfe, P. The physiological equivalent temperature—A universal index for the biometeorological assessment of the thermal environment. *Int. J. Biometeorol*. **1999**, *43*, 71–75. [[CrossRef](#)]
51. Matzarakis, A.; Mayer, H.; Iziomon, M. Applications of a universal thermal index: Physiological equivalent temperature. *Int. J. Biometeorol*. **1999**, *43*, 76–84. [[CrossRef](#)] [[PubMed](#)]

52. Hasan, M.H.; Alsaleem, F.; Rifaie, M. Sensitivity study for the PMV thermal comfort model and the use of wearable devices biometric data for metabolic rate estimation. *Build. Environ.* **2016**, *110*, 173–183. [[CrossRef](#)]
53. Senevirathne, D.; Jayasooriya, V.; Dassanayake, S.; Muthukumaran, S. Effects of pavement texture and colour on Urban Heat Islands: An experimental study in tropical climate. *Urban Clim.* **2021**, *40*, 101024. [[CrossRef](#)]
54. Cheung, P.K.; Jim, C. Comparing the cooling effects of a tree and a concrete shelter using PET and UTCI. *Build. Environ.* **2018**, *130*, 49–61. [[CrossRef](#)]
55. Lin, T.-P.; Matzarakis, A.; Hwang, R.-L. Shading effect on long-term outdoor thermal comfort. *Build. Environ.* **2010**, *45*, 213–221. [[CrossRef](#)]
56. Yang, J.; Hu, X.; Feng, H.; Marvin, S. Verifying an ENVI-met simulation of the thermal environment of Yanzhong Square Park in Shanghai. *Urban For. Urban Green.* **2021**, *66*, 127384. [[CrossRef](#)]
57. Tsoka, S.; Tsikaloudaki, A.; Theodosiou, T. Analyzing the ENVI-met microclimate model's performance and assessing cool materials and urban vegetation applications—A review. *Sustain. Cities Soc.* **2018**, *43*, 55–76. [[CrossRef](#)]
58. Cilek, M.U.; Cilek, A. Analyses of land surface temperature (LST) variability among local climate zones (LCZs) comparing Landsat-8 and ENVI-met model data. *Sustain. Cities Soc.* **2021**, *69*, 102877. [[CrossRef](#)]
59. Dong, B.; Shang, C.; Tong, M.; Cai, J. Analysis of the Influence of Age on Human Thermal Comfort. In Proceedings of the International Conference on Construction and Real Estate Management, Stockholm, Sweden, 24–25 August 2020.
60. Wu, Y.; Zhang, Z.; Liu, H.; Li, B.; Chen, B.; Kosonen, R.; Jokisalo, J. Age differences in thermal comfort and physiological responses in thermal environments with temperature ramp. *Build. Environ.* **2023**, *228*, 109887. [[CrossRef](#)]

Disclaimer/Publisher's Note: The statements, opinions and data contained in all publications are solely those of the individual author(s) and contributor(s) and not of MDPI and/or the editor(s). MDPI and/or the editor(s) disclaim responsibility for any injury to people or property resulting from any ideas, methods, instructions or products referred to in the content.